NEOPLASIA
www.neoplasia.com

Volume 17 Number 1 January 2015 pp. 32–42 32

Recombinant Interleukin-1 Receptor Antagonist Conjugated to Superparamagnetic Iron Oxide Nanoparticles for Theranostic Targeting of Experimental Glioblastoma[1,2,3]

Maxim A. Shevtsov[*,†], Boris P. Nikolaev[‡], Ludmila Y. Yakovleva[‡], Anatolii V. Dobrodumov[§], Alexander V. Zhakhov[‡], Anastasiy L. Mikhrina[¶], Emil Pitkin[#], Marina A. Parr[**], Valerii I. Rolich[**], Andrei S. Simbircev[‡] and Alexander M. Ischenko[‡]

*Institute of Cytology of the Russian Academy of Sciences (RAS), St. Petersburg, Russia; †A.L. Polenov Russian Research Scientific Institute of Neurosurgery, St. Petersburg, Russia; ‡Research Institute of Highly Pure Biopreparations, St. Petersburg, Russia; §Institute of Macromolecular Compounds of the Russian Academy of Sciences (RAS), St. Petersburg, Russia; ¶I.M. Sechenov Institute of Evolutionary Physiology and Biochemistry of the Russian Academy of Sciences (RAS), St. Petersburg, Russia; #Wharton School, University of Pennsylvania, Philadelphia, PA, USA; **V.F. Fock Institute of Physics, St. Petersburg State University, St. Petersburg, Russia

Abstract

Cerebral edema commonly accompanies brain tumors and contributes to neurologic symptoms. The role of the interleukin-1 receptor antagonist conjugated to superparamagnetic iron oxide nanoparticles (SPION–IL-1Ra) was assessed to analyze its anti-edemal effect and its possible application as a negative contrast enhancing agent for magnetic resonance imaging (MRI). Rats with intracranial C6 glioma were intravenously administered at various concentrations of IL-1Ra or SPION–IL-1Ra. Brain peritumoral edema following treatment with receptor antagonist was assessed with high-field MRI. IL-1Ra administered at later stages of tumor progression significantly reduced peritumoral edema (as measured by MRI) and prolonged two-fold the life span of comorbid animals in a dose-dependent manner in comparison to control and corticosteroid-treated animals ($P < .001$). Synthesized SPION–IL-1Ra conjugates had the properties of negative contrast agent with high coefficients of relaxation efficiency. *In vitro* studies of SPION–IL-1Ra nanoparticles demonstrated high intracellular incorporation and absence of toxic influence on C6 cells and lymphocyte viability and proliferation. Retention of the nanoparticles in the tumor resulted in enhanced hypotensive T_2-weighted images of glioma, proving the application of the conjugates as negative magnetic resonance contrast agents. Moreover, nanoparticles reduced the peritumoral edema confirming the therapeutic potency of synthesized conjugates. SPION–IL-1Ra nanoparticles have an anti-edemal effect when administered through a clinically relevant route in animals with glioma. The SPION–IL-1Ra could be a candidate for theranostic approach in neuro-oncology both for diagnosis of brain tumors and management of peritumoral edema.

Neoplasia (2015) 17, 32–42

Address all correspondence to: Dr M. A. Shevtsov, MD, PhD, Institute of Cytology (RAS), 194064 Tikhoretsky Ave. 4, St. Petersburg, Russia.
E-mail: shevtsov-max@mail.ru

[1] This article refers to supplementary materials, which are designated by Supplementary Materials 1 to 5 and are available online at www.neoplasia.com.

[2] Conflict of interest statement: None declared.

[3] Funding: This work was supported by grants from the Russian Foundation for Basic Research (No. 140800614 and No. 130401299), a grant from the Program of Molecular and Cellular Biology (RAS), and a government grant (20.11.2012; No. 14. N08.11.0001).
Received 10 September 2014; Revised 28 October 2014; Accepted 3 November 2014

1476-5586/15
http://dx.doi.org/10.1016/j.neo.2014.11.001

Introduction

Peritumoral brain edema is one of the most common complications of malignant brain tumor growth that contribute to neurologic deficits. Moreover, as was shown by Schoenegger et al., edema represents an independent prognostic factor for overall survival of patients with high-grade glioma [1]. Thus, patients with major edema [>1 cm on preoperative magnetic resonance imaging (MRI)] had significantly shorter overall survival compared to patients with minor edema (<1 cm) [1]. The "gold standard" treatment of peritumoral edema is corticosteroid therapy that is associated with numerous serious side effects [2,3].

The large number of complications has led to the discovery of alternative approaches in the reduction of peritumoral edema in neuro-oncological patients. Several up-to-date agents were proposed, including corticotropin releasing factor, cyclooxygenase-2 inhibitors, and inhibitors of vascular endothelial growth factor (VEGF) [i.e., anti-VEGF antibodies (bevacizumab) and inhibitors of VEGF receptors (cediranib)] [4,5]. Implication of anti-angiogenic agents (e.g., bevacizumab) that were shown to exert anti-edemal effect is limited due to their high cost [6]. Application of the osmotherapy such as diuretic bumetadine was also shown to decrease the peritumoral edema, thus prolonging the life span of glioma-bearing animals [7]. Though there is a well-documented reduction in brain edema, an adverse rebound increase of intracranial pressure is observed after its withdrawal. Nevertheless, osmotherapy could be applied as a temporary measure to acutely prevent brain stem compression [8].

An alternative approach could be based on the application of the interleukin-1 receptor antagonist (IL-1Ra). Previously, it was demonstrated by Masada et al. that IL-1Ra significantly reduced brain edema in the experimental model of intracerebral hemorrhage, probably through reduction of thrombin-induced brain inflammation [9,10]. In another study by Tehranian et al., IL-1Ra was shown to modulate expression of pro-inflammatory cytokines (i.e., IL-1 and tumor necrosis factor alpha [TNFα]) in the model of head injury in mice [11]. Blockage of IL-1 signaling had a neuroprotective effect and improved the neurologic recovery after traumatic brain injury. Moreover, administration of IL-1Ra proved to reduce inflammatory response in the animal models of brain ischemia [12–14]. In the study by Pradillo et al., rats following transient (90 minutes) occlusion of the middle cerebral artery were administered two doses of IL-1Ra (25 mg/kg, subcutaneously) during reperfusion [13]. Injection of IL-1Ra significantly reduced infarct volume (as measured by MRI), microglial activation, neutrophil infiltration, and cytokine levels in the brain [13]. All the data collected to date indicate that IL-1Ra has a significant anti-edemal and anti-inflammatory effect in various animal models and thus might be beneficial in reduction of peritumoral edema in brain tumors. Moreover, according to several studies, IL-1Ra also possesses a therapeutic anti-tumor effect [14–16]. Thus, it was demonstrated by Bar et al. that administration of the antagonist in the model of fibrosarcoma in mice significantly reduced the tumor progression and increased the survival rates [14]. One hypothesis for the inhibition of tumor growth is that IL-1Ra blocks IL-1 receptors in cancer cells, thus reducing the proliferative and angiogenic effects of IL-1 [15]. There is also evidence that IL-1Ra downregulates IL-8 that plays a central role in cancer growth [15,17].

In the present study, the anti-edemal effect of IL-1Ra systemically administered was assessed in the model of intracranial glioma in rodents. In addition, IL-1Ra activity was analyzed as related to the glioma progression and overall survival of tumor-bearing animals. Following analysis of the therapeutic potency of IL-1Ra, a novel theranostic agent based on superparamagnetic iron oxide nanoparticles (SPIONs) was developed. We also report that an engineered conjugate of SPIONs with IL-1Ra can be applied for diagnosis of tumors as well as for reduction of peritumoral edema.

Materials and Methods

Preparation and Purification of Recombinant IL-1Ra

IL-1Ra was produced by recombinant gene technology from *Escherichia coli* BL21 in solution (99% purity) by State Research Institute of Highly Pure Biopreparations (St. Petersburg, Russia). Quantitation of endotoxin was performed using the *Limulus amoebocyte* lysate assay (QCL-1000; Cambrex Bio Science, Walkersville, MD). The resulting endotoxin content was below 0.1 EU/mg IL-1Ra. Biologic activity of IL-1Ra was assessed in the test of inhibition of induced IL-8 production by T98 and U118 glioma cells (Supplementary Material 1) and analysis of mice thymocyte proliferation assay (Supplementary Material 2).

Analysis of the Anti-Edemal Activity of IL-1Ra and Animal Survival Analysis

Cells. The C6 rat glioma cell line was obtained from the Russian Cell Culture Collection at the Institute of Cytology, Russian Academy of Sciences (St. Petersburg, Russia). C6 cells were grown in Dulbecco's modified Eagle's medium/F12 medium supplemented with 10% FBS, 2 mM L-glutamine, and antibiotics (100 U/ml penicillin G and 0.1 mg/ml streptomycin). Cells were grown in a CO_2 incubator with 6% CO_2 and 90% humidity. Viability was determined by 0.4% trypan blue exclusion.

Orthopic model of C6 glioma. Male Wistar rats weighing 250 to 300 g were purchased from an animal nursery ("Rappolovo" RAMN, St. Petersburg, Russia). Animals were anesthetized before mounting in a stereotactic frame (David Kopf Instruments, Tujunda, CA) with 10 mg of "Zoletyl-100" (tiletamine hydrochloride and zolazepam; "Virbac santé Animale", Carros cedex, France) and 0.2 ml of 2% Rometar (xylazinum hydrochloride; "Bioveta", Ivanovice na Hané, Czech Republic) intraperitoneally. C6 glioma cells (1×10^6 cells/ml) resuspended in 10 μl of phosphate-buffered saline (PBS) were injected into the *nucl. caudatus dexter*. All animal experiments were approved by the local ethical committee of the Institute of Cytology (RAS) (St. Petersburg, Russia) in compliance with the US Department of Health and Human Services Guide for the Care and Use of Laboratory Animals (1996).

Analysis of IL-1Ra penetration through the blood-tumor barrier. For assessment of the IL-1Ra retention in the C6 glioma, the protein was intravenously (i.v.) administered on the 25th day following tumor inoculation (50 mg/kg). After 24 hours, the animals were sacrificed, and their brains were extracted and fixed in 10% formaldehyde. IL-1Ra was revealed with the help of anti–IL-1Ra mice monoclonal antibodies (Cytokin, St. Petersburg, Russia) and secondary Alexa Fluor 555–conjugated antibodies (Invitrogen, Carlsbad, CA). Nuclei were stained with DAPI (4′,6-diamidino-2-phenylindole). Brain sections were analyzed with the help of Leica SP5 confocal microscopy (Leica Microsystems, Heidelberg, Germany).

Animal survival analysis. To assess the effects of the i.v. infused IL-1Ra on the survival of the tumor-bearing animals, the experiments were performed according to the following schedule: the first group of rats received saline solution (n = 20), the second group of animals was injected with BSA at 100 mg/kg (n = 20), the third, fourth, and fifth groups (n = 20) were injected with IL-1Ra at 25, 50, and 100 mg/kg, respectively, and the sixth group (n = 20) received dexamethasone (4 mg/kg) i.v. and was used as a positive control. Following intracranial implantation of the C6 glioma cells on the 15th day, animals were randomly divided into six groups. Animals received a course of five

i.v. injections through the tail vein on the 15th, 17th, 19th, 21st, and 23rd day after the inoculation of the C6 cells. The animal's survival was estimated according to the Kaplan-Meier method.

MR assessment of the tumor volume and peritumoral edema. MRI was used to measure the cerebral edema following treatment with IL-1Ra. On the 15th day following glioma implantation, animals were randomly divided into six groups (three animals each) as follows: control group (infusion of the saline solution), group treated with dexamethasone (4 mg/kg), BSA-treated groups, and experimental groups with i.v. administration of IL-1Ra at 25, 50, and 100 mg/kg, respectively. Twenty-four hours after injection, animals were assessed with multiple MRI modalities. MR sequences were obtained at the following regimens: TurboRARE-T2, RARE-T1, FLASH, multi-slice multi-echo (MSME), and diffusion-weighted image (DWI). Tumor volume on T_1-weighted and T_2-weighted MR scans was calculated by measuring the cross-sectional areas on each MR slice and multiplying their sum by the slice thickness. Peritumoral edema was defined as a region of increased T_2 signal intensity on the tumor margin. In the perifocal lesion area, the apparent diffusion coefficient (ADC) value was assessed. ADC values were calculated according to the following formula: ADC = $-1(1/b)\ln(S/S_0)$, where S and S_0 were the signal intensities in the region of interest (ROI) that was obtained with various gradient factors (b values of 0 and 1000 s/mm^2). The ROI was placed in the C6 glioma and normal brain area on the ADC map. Each ROI was positioned twice with a change of location, and ADC values were averaged. ADC values of the animals from the control group and those of the animals treated with BSA, dexamethasone, and IL-1Ra at 25, 50, and 100 mg/kg were compared. Three animals were allocated for each group. ADC values were obtained on the 14th, 20th, 25th, and 30th day following C6 glioma inoculation.

Synthesis of Magnetic Nanoparticles Conjugated with IL-1Ra

Recombinant IL-1Ra was conjugated with SPIONs as described earlier [15]. Briefly, SPIONs were prepared from iron salt solutions by co-precipitation in alkaline media at 80°C. $FeSO_4$ and $FeCl_3$ at an Fe^{2+}/Fe^{3+} ratio of 1:2 were dissolved in water with the addition of CsCl. Magnetite precipitation was induced by titration with an NH_4OH solution in an inert atmosphere under vigorous stirring in a 100-ml reactor. The precipitate was collected by a permanent magnet. To prevent sedimentation, low molecular weight dextran (MW 10 kDa; Sigma, St. Louis, MO) was added to the dispersion during the process of ultrasound application. The prepared stock solution of nanoparticles was washed and separated into fractions by centrifugation and microfiltration using 0.2-μm pore membranes (Millipore, Billerica, MA). The Fe content in the suspension was controlled by UV absorption of the thiocyanate-Fe(+3) complex at λ = 480 nm. For conjugation with IL-1Ra, the dextran coating on the magnetic nanoparticles was cross-linked with epichlorohydrin and aminated. Magnetic nanoparticles were suspended in a phosphate-buffered solution of IL-1Ra (60 μg/ml). The conjugation reaction was carried out at 20°C with shaking for 1 hour. Soluble carbodiimide dextran was activated by water and coupled to the carboxyl groups of IL-1Ra, producing a magnetic conjugate. The specific immune activity of the synthesized SPION–IL-1Ra conjugates was estimated by a magnetic relaxation switch assay [16,17]. The Fe content in the magnetic IL-1Ra conjugate samples was analyzed by spectrophotometry of the thiocyanate-Fe(+3) complex, prepared by HNO_3 dissolution. The IL-1Ra content in conjugate samples was measured using a human IL-1Ra ELISA kit (Protein Contour, St. Petersburg, Russia).

The particle size and size distribution of SPIONs and its conjugates were studied by transmission electron microscopy (TEM) using a JEOL-2000 microscope (JEOL, Akishima, Tokyo, Japan) and dynamic light scattering (DLS) (Supplementary Material 3) using a Malvern instrument. The hydrodynamic size and electrophoretic properties were measured on Zetasizer Nano (Malvern, Worcestershire, United Kingdom). NMR spectra and magnetic relaxation times, i.e., T_1, T_2, and T_2, were measured using CXP-300, an nuclear magnetic resonance (NMR) spectrometer (Bruker, Billerica, MA), with a magnetic field of 7.1 T. To estimate the magnetic relaxation times, the inversion recovery and Carr-Purcell-Meiboom-Gill impulse sequences were applied. Proton relaxation times were studied as a function of the magnetic IL-1Ra conjugate concentration in a buffered solution. The coefficients of relaxation efficiency, i.e., R_1, R_2, and R_2 (relaxivity), were determined from the slopes of the concentration plots.

Assessment of C6 Cells and Lymphocyte Uptake of SPION–IL-1Ra

In the series of *in vitro* experiments, the IL-1Ra conjugates were added to the C6 glioma cell culture for 6, 12, and 24 hours (Fe concentration of 150 μg/ml). Following incubation, cells were washed, fixed, and analyzed with the help of confocal microscopy on a Leica DM IRBE microscope (Leica Microsystems) by reflecting laser scanning for SPION–IL-1Ra distribution inside the C6 cells. The uptake of the conjugates was also analyzed in rat lymphocytes. Cells were isolated from the peripheral blood mononuclear cells obtained by Ficoll density gradient centrifugation. Additionally, cells were purified from monocytes by adherence as described elsewhere [22]. Following purification, cells were incubated with SPION or SPION–IL-1Ra for 6, 12, and 24 hours and assessed for distribution of nanoparticles with the help of confocal microscopy, as was described earlier. The localization of the conjugates in the cells was assessed by TEM. Briefly, following incubation with SPION or SPION–IL-1Ra conjugates for 24 hours, cells were detached with trypsin/EDTA from the culture plate, fixed in 2.5% glutaraldehyde in 0.1 M cacodylate buffer, pH 7.4, for 1 hour at 4°C, postfixed in 1% aqueous OsO_4 for 1 hour, dehydrated, and embedded in Epon and Araldite, and then sectioned with a diamond knife on an LKB ultratome. Ultrathin sections were collected on fine mesh copper or nickel grids and stained with uranyl acetate and lead citrate for examination with Zeiss Libra 120 electron microscope operated at 80 kV.

Assessment of Tumor Targeting with SPION–IL-1Ra Conjugates

To assess the accumulation of IL-1Ra conjugated with SPION in C6 gliomas, animals were randomly divided into three groups (three animals each) on the 25th day after C6 cell administration: 1) i.v. injection of PBS (control group); 2) i.v. injection of SPION (300 μl, 0.3 mg/kg) for 24 hours; 3) i.v. injection of SPION–IL-1Ra conjugates (300 μl, 0.3 mg/kg) for 24 hours. Assessment was performed using a high-field 11-T MRI scanner (Bruker) with a custom rat coil. High-resolution anatomic T_2-weighted scans [repetition time (TR)/echo time (TE) 4200/36 milliseconds, flip angle 180°, slice thickness 1.0 mm, interslice distance 1.2 mm, field of vision 2.5 × 2.5 cm, matrix 256 × 256, in total 20 slices] were performed in the coronal plane. Additionally, we performed T_1-weighted scans (TR/TE 1500/7.5 milliseconds, flip angle 180°, slice thickness 1.0 mm, field of vision 2.5 × 2.5 cm, matrix 256 × 256) and FLASH scans (TR/TE 350/5.4 milliseconds, flip angle 40°, slice thickness 1.0 mm, 2.5 × 2.5 cm, matrix 256 × 256) in the coronal plane. For an estimation of the

accumulation of nanoparticles in the tumor, we used MSME MR sequences. The obtained images were analyzed using Analyze software (AnalyzeDirect, Inc, Overland Park, KS). The MSME images were used to generate T_2 maps over the tumor region. For a calculation of the tumor contrast enhancement on the T_2 maps, we applied the software package Paravision 3.1 (Bruker BioSpin GmbH, Rheinstetten, Germany). We displayed the histogram and calculated the mean and SD of the T_2 values of the tumor. Retention of the IL-1Ra conjugates in the tumor was further confirmed with the histologic analysis of the tumor samples. Following injection of the conjugates, the rats were sacrificed, and tumors were extracted and fixed overnight in 10% formalin. Tissues were then embedded in Tissue-Tek and stored at −80°C. Sections (5-7 μm thick) prepared from these blocks were mounted on SuperFrost Plus slides (Fischer Scientific, Hampton, NH) and used for the detection of magnetic conjugates through confocal microscopy. Sections were additionally stained with DAPI. Fluorescence images were obtained using a Leica TCS SP5 confocal system. SPIONs or SPION–IL-1Ra conjugates were detected by reflecting laser scanning with laser excitation at 488 nm (Ar/Kr). Nuclei were detected using a diode laser (405 nm).

For survival analysis, animals were randomly divided on the 14th day in five groups (10 rats each) as follows: control, BSA treated, dexamethasone treated (4 mg/kg), SPION treated, and SPION–IL-Ra treated at 1.25 and 2.5 mg/kg of total IL-1Ra per treatment course.

Statistical Analysis

Kaplan-Meier survival curves were plotted for the five groups of animals treated with saline solution, dexamethasone, or IL-1Ra at various concentrations. Two-tailed Student's t tests were used to evaluate the differences between control and experimental groups. All data were analyzed with Statistica Version 9.2 for Windows and with the R statistical computing program. P values of $<.05$ were considered statistically significant for all tests.

Results

IL-1Ra Penetrates the Blood-Tumor Barrier and Exerts an Anti-Edemal Activity

Following i.v. injection of IL-1Ra, the accumulation of protein was assessed in the C6 glioma with the help of confocal microscopy (Figure 1). Twenty-four hours after infusion, IL-1Ra could be detected in the glioblastoma cells throughout the tumor. High magnification demonstrated the cytoplasmic localization of the IL-1Ra. Tumor retention of the antagonist had a significant influence on the peritumoral brain edema. The mean ADC value of the C6 glioma from the control group was $2.28 \pm 0.11 \times 10^{-3}$ mm^2/s (Supplementary Material 4). The mean ADC value did not significantly change in all studies with a slight increase up to day 30 (Figure 2). Application of the BSA as a control protein also did not influence the ADC parameter, equaling on the 30th day $2.77 \pm 0.08 \times 10^{-3}$ mm^2/s. Intravenous injection of the dexamethasone resulted in the decrease of the ADC value on the 20th day in comparison to the control and BSA-treated animals ($P < .001$). Thus, on the 20th and 25th days, the ADC values were $1.77 \pm 0.08 \times 10^{-3}$ and $1.44 \pm 0.09 \times 10^{-3}$ mm^2/s, respectively. Intriguingly, following cessation of dexamethasone treatment on the 23rd day, on the 30th day the ADC values started to increase and were $2.75 \pm 0.23 \times 10^{-3}$ mm^2/s. The subsequently obtained ADC maps for the treated animals also proved the dexamethasone effect (Figure 3*A*). When recombinant IL-1Ra was applied at 25 mg/kg on the 20th day, the decrease of the ADC value was comparable to that of the dexamethasone-treated group—$1.72 \pm 0.05 \times 10^{-3}$ mm^2/s. Further, IL-1Ra therapy resulted in the gradual decrease of the ADC value. On the 30th day, the anti-edemal effect was still observed—$1.40 \pm 0.05 \times 10^{-3}$ mm^2/s in comparison to the dexamethasone-treated group ($P < .001$). A statistically significant difference in ADC values was observed when the IL-1Ra at 50 and 100 mg/kg was administered. There was a significant decrease of edema in the glioma tissue as well as of peritumoral edema (Figure 3*A*). Thus, at 20th day, the ADC values were considerably lower than in dexamethasone- and IL-1Ra (25 mg/kg)–treated groups, equaling $1.07 \pm 0.09 \times 10^{-3}$ and $0.69 \pm 0.10 \times 10^{-3}$ mm^2/s, respectively ($P < .001$). The ADC values continued to be low for all periods of treatment and, at 30th day, were still significantly lower in comparison to other groups—$0.68 \pm 0.03 \times 10^{-3}$ (for 50 mg/kg) and $0.57 \pm 0.04 \times 10^{-3}$ (for 100 mg/kg) mm^2/s, respectively.

Intravenous Administration of IL-1Ra Reduces the Tumor Growth and Increases the Overall Survival of Tumor-Bearing Rats

In vivo studies showed the feasibility and safety of systemic delivery of the antagonist. We did not observe any side effects (i.e., behavioural changes) after infusion of IL-1Ra. According to the MR data on the 14th day following tumor inoculation, the mean tumor volume in the

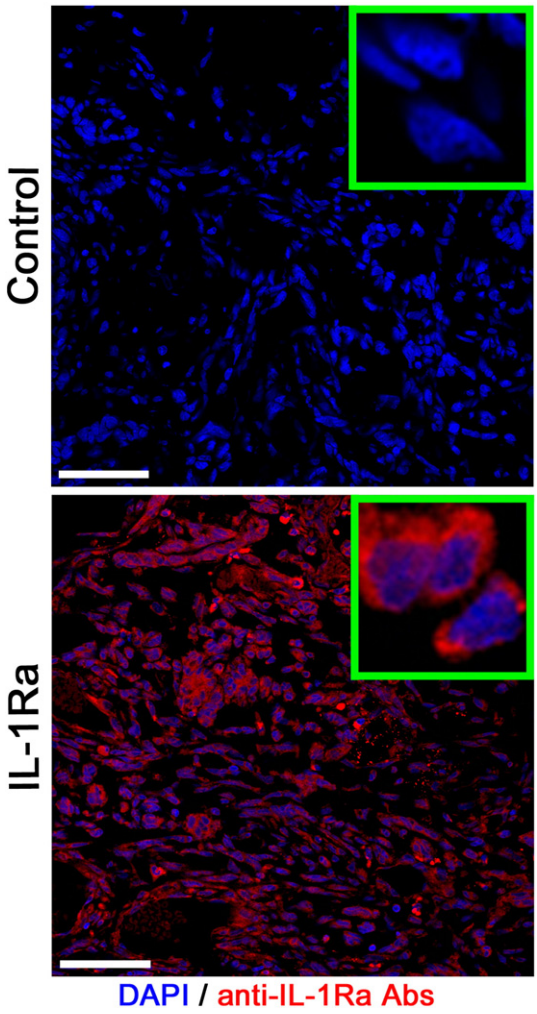

Figure 1. Confocal microscopy of the C6 glioma following i. v. administration of the IL-1Ra. Nuclei were stained with DAPI (blue). IL-1Ra was detected with monoclonal antibodies conjugated with Alexa Fluor 555 (red). Scale bar, 75 μm.

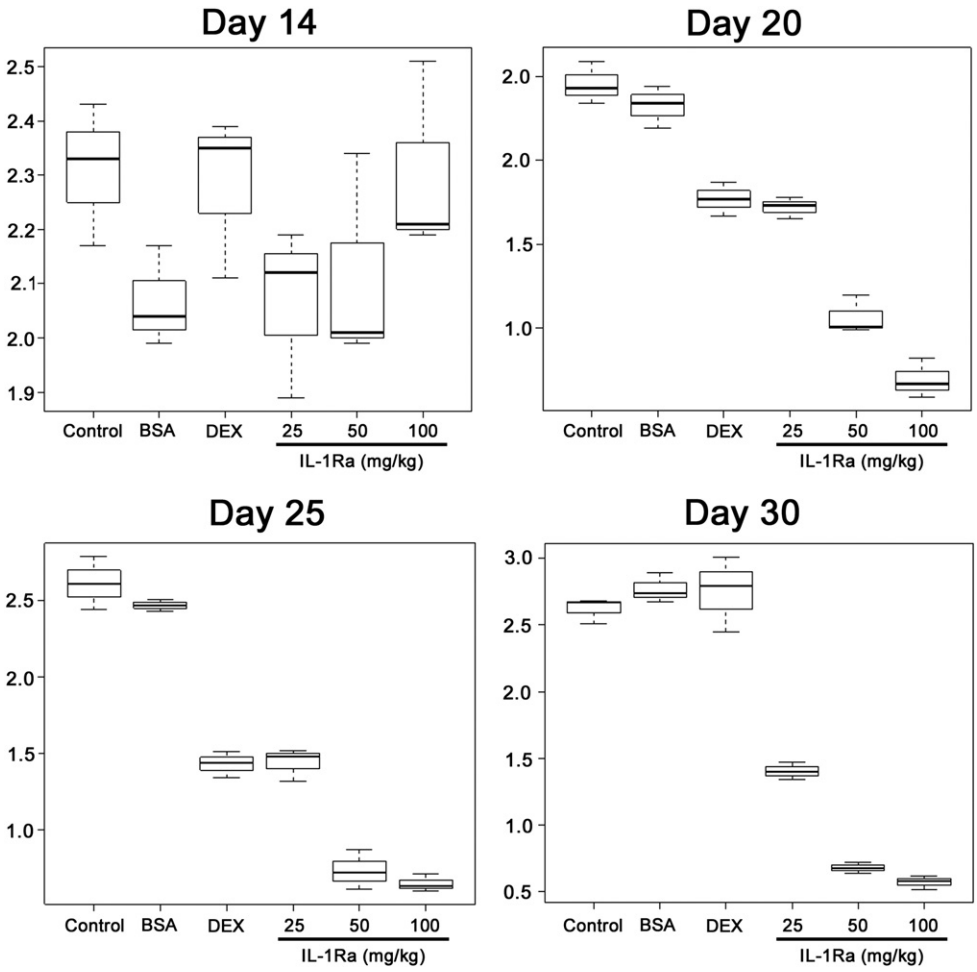

Figure 2. Side-by-side boxplots of ADC. ADC was calculated for the five experimental groups and for the control group on days 14, 20, 25, and 30 following C6 glioma cell inoculation.

control group was 184.49 ± 5.51 mm^3 (Supplementary Material 5). The exponential tumor growth was observed in control and BSA-treated groups, and at day 28, the tumor was 547.21 ± 64.29 and 590.19 ± 21.88 mm^3, respectively (Figure 3*B*). Dexamethasone administration resulted in the decrease of the tumor progression. Thus, on the 28th day, the glioma volume was 342.46 ± 31.65 mm^3, and only after the cessation of the corticosteroid therapy did the tumor growth continue to increase, equaling on the 42nd day 588.52 ± 13.83 mm^3 ($P < .001$). The effect of IL-1Ra infusion at 25 mg/kg was comparable to that of dexamethasone with a mean tumor volume on the 28th day of 350.53 ± 11.29 mm^3. Further increase of antagonist concentration resulted in significant delay of tumor progression. Following the end of IL-1Ra infusions on the 23rd day, the delay of the glioma growth was still obvious, constituting 396.43 ± 13.48 (IL-1Ra, 50 mg/kg) and 338.20 ± 6.65 (100 mg/kg) mm^3.

Intravenous delivery of the IL-1Ra prolonged the life span of rats in the experimental groups in a dose-dependent manner (Figure 3*C*). Accordingly, in the IL-1Ra–treated group at 50 mg/kg, the survival was increased two-fold in comparison to the control and BSA-treated groups, equaling 41.5 ± 11.9, 23.9 ± 3.4 and 23.2 ± 3.4 days, respectively ($P < .001$). Further increase of the concentration of the infused IL-1Ra to 100 mg/kg resulted in elevation of the survival up to 51.3 ± 15.6 days ($P < .001$). Application of dexamethasone as a positive control resulted in the slight but statistically significant increase in rats' survival compared to control—36.9 ± 8.2 days ($P < .001$). The efficacy of the corticosteroid therapy was comparable to the injection of IL-1Ra at 25 mg/kg. However, application of the antagonist at higher doses (i.e., 50 and 100 mg/kg) demonstrated an increase in animals' survival that dramatically exceeded the survival in the corticosteroid-treated group.

Synthesized SPION–IL-1Ra Conjugates Exert the Properties of the Negative MR Contrast Agent

The prepared magnetic conjugates of IL-1Ra appeared to have the typical characteristics of SPIONs known for different magnetic nanodispersions of various compositions. According to DLS measurements, the conjugate solutions have a colloidal structure consisting of iron oxide nanoparticles coated by dextran with a coupled receptor antagonist. The measured hydrodynamic radius of non-conjugated SPIONs was 37.9 nm (Figure 4*A*). The IL-1Ra conjugation increased the mean size of the nanoparticles to 43.1 nm. The measured zeta potential of the SPION–IL-1Ra was 13.8 mV (Figure 4*B*). The presence of IL-1Ra in the nanoparticles was assessed with the DLS assay (Figure 4*C*). Addition of the anti-IL-1Ra monoclonal antibodies resulted in a significant increase of the nanoparticles' size that was not observed if control isotype IgG antibodies were applied. SPION–IL-1Ra conjugate solutions exhibited the properties of negative contrast enhancement as was demonstrated by NMR data (Figure 5). Magnetic relaxation study of SPION–IL-1Ra nanoparticles proves the strong

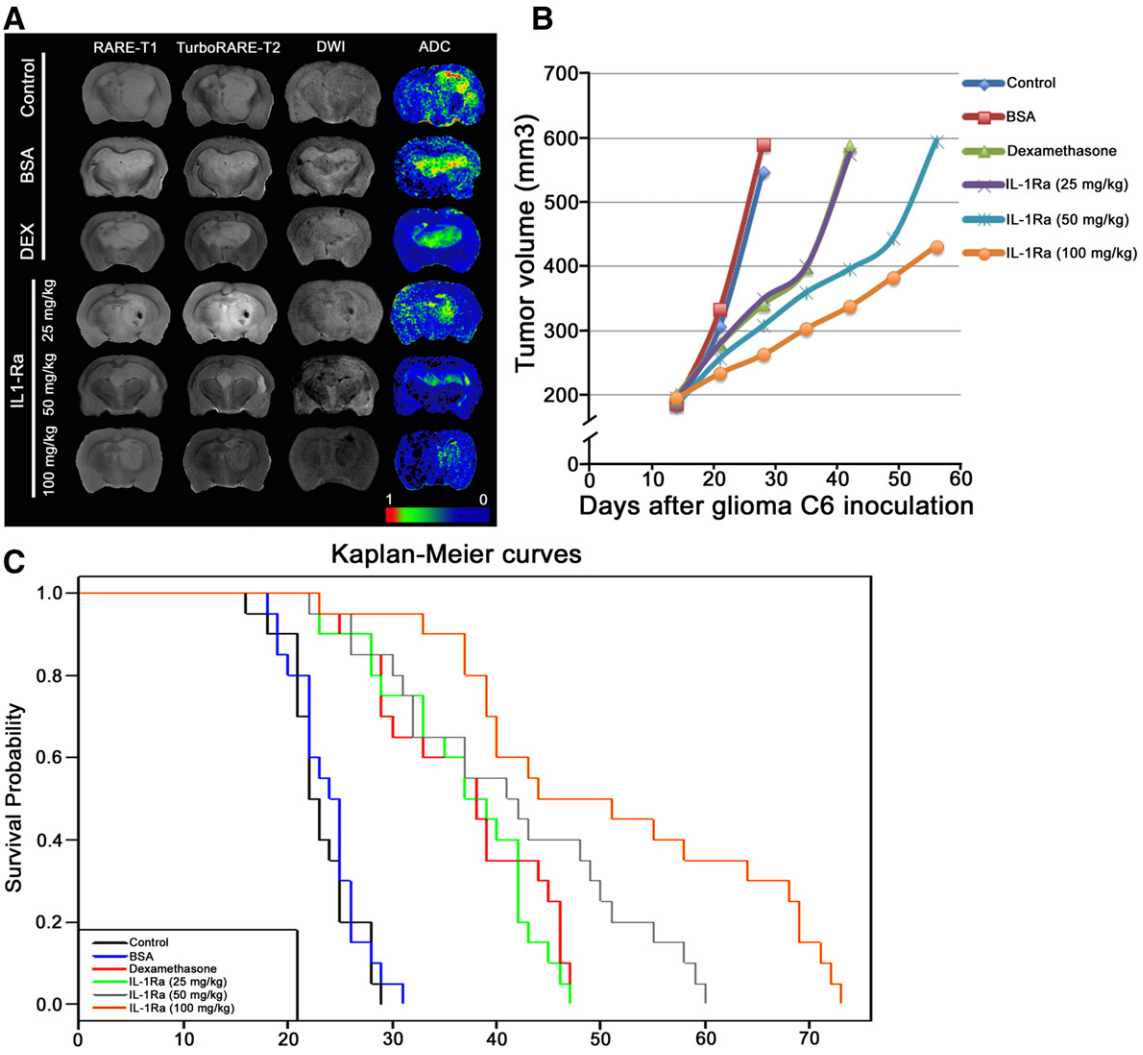

Figure 3. Anti-edemal activity of recombinant IL-1Ra and animal survival analysis. (A) MRI of the C6 glioma at day 25 for the animals from control and treated with BSA, dexamethasone (DEX), and IL-1Ra at 25, 50, and 100 mg/kg. MR scans were obtained at RARE-T1, TurboRARE-T2, and DWI regimens. Additionally for each animal, the ADC map was calculated. (B) Tumor volume growth dynamics (mm^3) for animals from five experimental groups and control group. (C) Kaplan-Meier survival curves for control and experimental groups.

influence of MR relaxation of water protons from the presence of iron oxide magnetic core in dispersion. The magnetic relaxation behavior had a dose-dependent character. The decrease of magnetic relaxation times T_1, T_2, and T_2 was in linear dependence on the iron content in suspension measured by UV absorbance of thiosulfate coordination complex. The values of relaxation efficiency were calculated as derivative coefficients of linear plots of concentration dependences.

Accumulation of the SPION–IL-1Ra Nanoparticles in C6 Cells and Lymphocytes

Toxicity analysis that included C6 proliferation assessment by exclusion of the trypan blue and dye 3-(4,5-dimethylthiazol-2-yl)-2,5-diphenyltetrazolium bromide (MTT) assay, measured by relative viability, clearly demonstrated the absence of toxic effects of SPIONs or SPION–IL-1Ra conjugates (at the range of Fe concentrations from 150 to 350 μg/ml). The cell viability did not differ at any time points of incubation (1, 3, 12, and 24 hours) with SPIONs or SPION–IL-1Ra nanocarriers, and it was not different from control cells. Further, the incorporation of the nanoparticles into the C6 cells was assessed (Figure 6*A*). Following 24 hours of incubation with SPIONs, the cytoplasmic incorporation of the particles by glioma cells was demonstrated. When SPION–IL-1Ra conjugates were applied, the amount of the included nanoparticles was significantly higher in comparison to the non-modified SPION. Subsequent addition of blocking monoclonal anti–IL-1R antibodies resulted in the reduction of the SPION–IL-1Ra being taken up by C6 cells, which indicates the possible mechanism of receptor-mediated endocytosis. Further immunocytochemistry demonstrated that SPION–IL-1Ra conjugates were co-localized with IL-1R in the endosome-like structures in the cytoplasm (Figure 6*B*). The confocal microscopy analyses of the SPIONs or SPION–IL-1Ra conjugates with rat lymphocytes clearly demonstrated the receptor-mediated mechanism of antagonist incorporation into the cells (Figure 6, *C* and *D*).

Retention of SPION–IL-1Ra in the Tumor Decreases the Peritumoral Edema and Prolongs the Life Span of Animals

All i.v. injections of SPION–IL-1Ra or SPIONs were well tolerated by the rats. We did not observe any side effects. The C6

glioma presented as hypotensive or isotensive on the T_1-weighted images and hypertensive on the T_2-weighted scans (Figure 7*A*). When non-conjugated SPIONs following 24 hours were applied, the retention of the nanoparticles was observed in the brain tumor as hypotensive zones on T_2-weighted images with a slight change in the T_2 values. When SPION–IL-1Ra conjugates were applied, a significant decrease in the T_2 signal in the zone of the tumor after 24 hours of injection in comparison to that of non-modified SPIONs or control non-treated animal was observed ($P < .001$). Antagonist magnetic conjugates accumulated throughout the glioma and presented as hypotense zones on the T_2-weighted images. Corresponding T_2 maps of the treated tumor calculated from the MSME images demonstrated decreased T_2 values. Confocal microscopy analysis of the tumor sections in the reflecting laser scanning confirmed the accumulation of the SPION–IL-1Ra conjugates in the C6 tumor (Figure 7*B*). Nanoparticles accumulated in the cytoplasm of the cells surrounding the nucleus. According to animal survival analysis, infusions of the IL-1Ra conjugates (of a total of 2.5 mg/kg IL-1Ra) also prolonged the survival of animals in comparison to the control and SPION-treated groups, amounting to 21.4 ± 4.1, 21.7 ± 3.7, and 41.5 ± 11.32 days, respectively ($P < .001$) (Figure 7*C*). Subsequent diffusion-weighted imaging and ADC maps demonstrated that tumor retention of the SPION–IL-1Ra conjugates resulted in the decrease of the peritumoral edema in comparison to the non-conjugated SPIONs (Figure 7*D*).

Discussion

Nanomedicine based on iron oxide magnetic nanoparticles functionalized with various bioligands has brought a paradigm shift in the diagnosis and treatment of malignant brain tumors [23,24]. Due to their unique properties, functionalized magnetic particles could be used both as negative MR contrast agents for tumor detection and carriers for tumor-targeted drug delivery [25]. This approach was tested for numerous combinations of bioligands and their receptors that are overexpressed in gliomas including Pep-1, a specific ligand for IL-13Rα2, antibodies for epidermal growth factor receptor deletion mutant, epidermal growth factor receptor vIII, Hsp70 for CD40 receptor, F3 peptide for nucleolin, and many others [19-21,26–28].

For the present study, a recombinant receptor antagonist for IL-1 (IL-1Ra) that was conjugated with magnetic nanoparticles (SPION–IL-1Ra) was applied. IL-1 isoforms (IL-1α and IL-1β) play roles in tumor progression, angiogenesis, and metastasis either directly or indirectly through induction of various cytokines [29]. Moreover, IL-1 also promotes myeloid-derived suppressor cells and M2-type macrophages that exert immunosuppression in the tumor site [30,31]. Thus, application of IL-1Ra might not only reduce tumor-induced edema but also influence the glioma growth. According to our data, we observed a dramatic accumulation of the recombinant IL-1Ra in the glioma tissue if i.v. administered (Figure 3). Previously, the IL-1Ra pharmacokinetics, biodistribution, and metabolism were studied using [^{18}F]–IL-1Ra and positron emission tomography (PET) imaging in rats [32]. The results of protein uptake exhibited slower pharmacokinetics in the normal brain due to the presence of the blood-brain barrier [32]. The retention of receptor antagonist in the glioma could be explained by the disrupted blood-brain barrier that characterizes the growth of malignant brain tumors [18,33–36].

In our studies, it was shown for the first time that recombinant IL-1Ra has a significant anti-edemal effect in the experimental brain tumor model (Figures 2 and 3). Systemic administration of IL-1Ra dramatically reduced the peritumoral edema in a dose-dependent manner. For analysis of edema, we applied the ADC that is used as a sensitive method for assessment of treatment response in neuro-oncology [37]. Intriguingly, we observed a decrease in ADCs for IL-1Ra–treated groups in comparison to control, BSA-treated, and dexamethasone-treated groups (Figure 2). Thus, on the 30th day following tumor inoculation, the ADC coefficient for the control group was 2.62 ± 0.08, while for IL-1Ra (100 mg/kg), it was 0.57 ± 0.04 ($P < .001$). The reduction of tumor-induced edema on DWIs and ADC

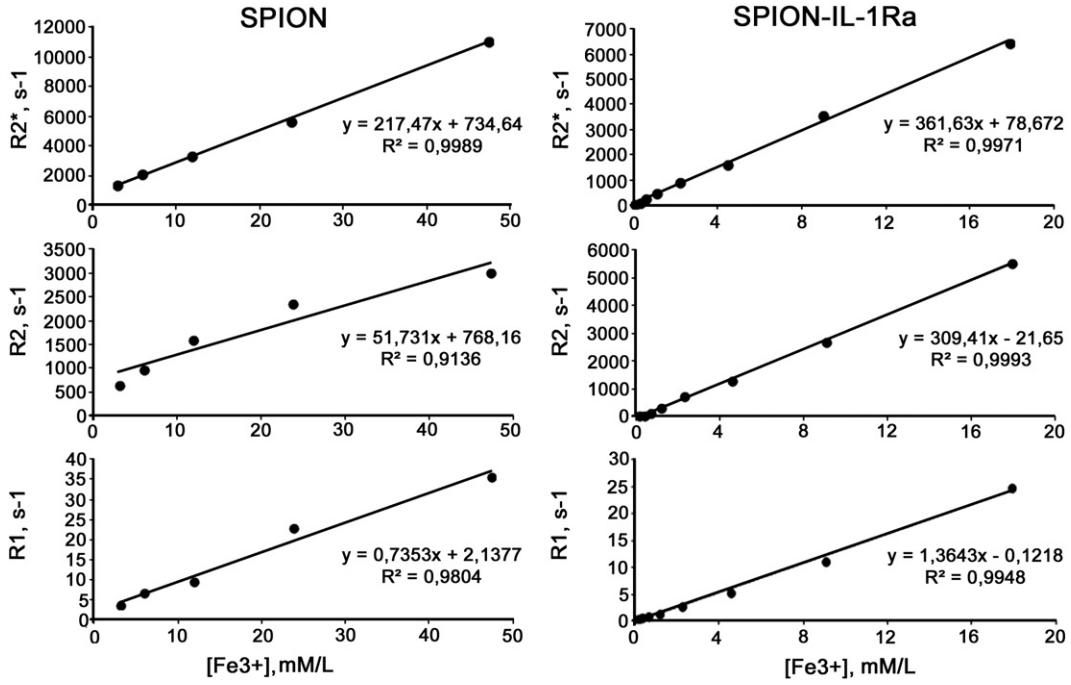

Figure 4. Magnetic relaxation rates R_2^*, R_2, and R_1 of water protons in SPIONs and SPION–IL-1Ra conjugate dispersion in dependence on the Fe concentration at 20°C.

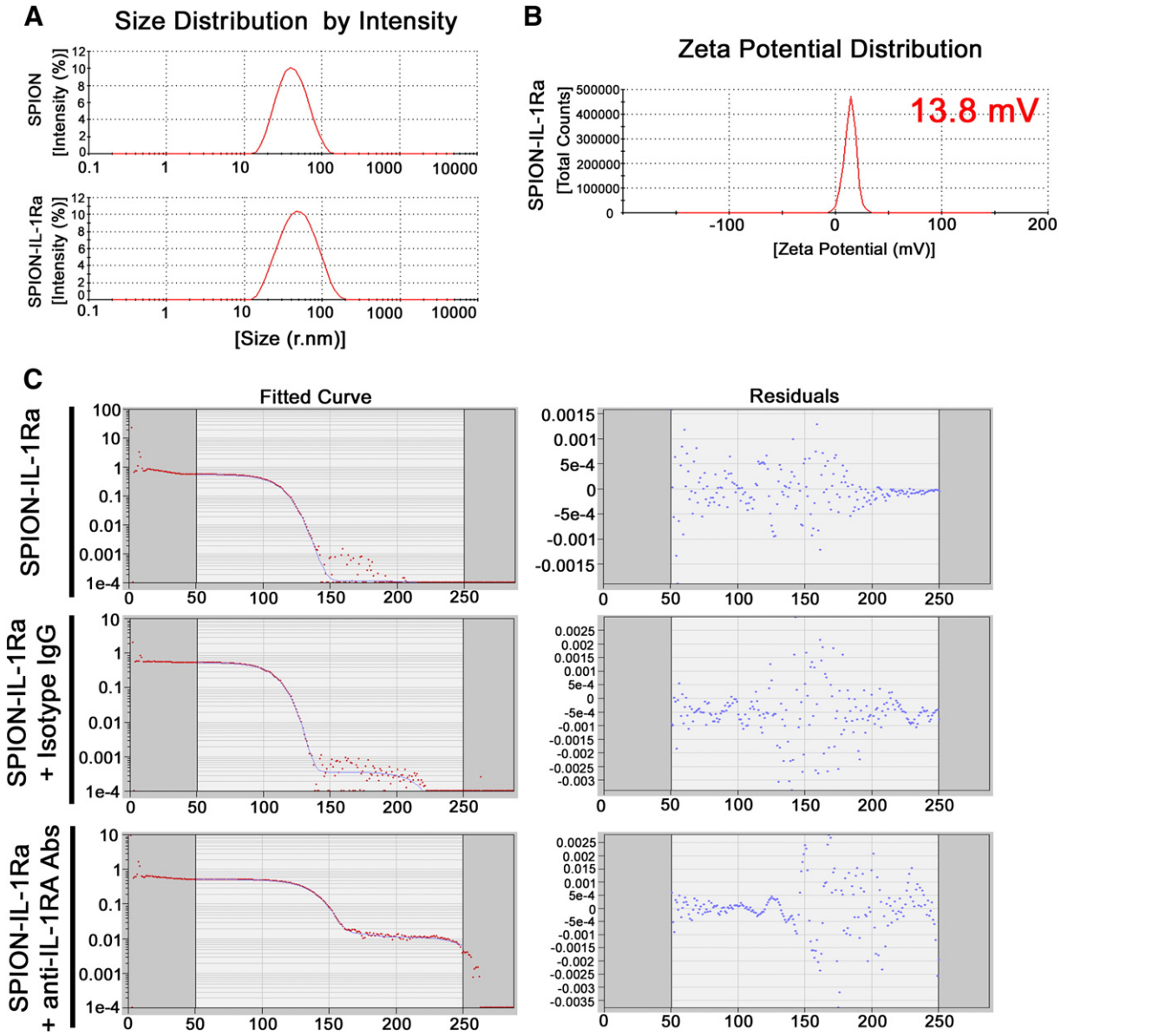

Figure 5. Characterization of the synthesized SPION–IL-1Ra conjugates. (A) Hydrodynamic size (r.nm) of the SPIONs and SPION–IL-1Ra nanoparticles. (B) Zeta potential for the SPION–IL-1Ra conjugates. (C) DLS assay for the SPION–IL-1Ra particles incubated with isotype IgG antibodies or monoclonal anti–IL-1Ra antibodies for 4 hours.

maps was comparable to that of anti-angiogenic treatment described earlier (e.g., bevacizumab, endostatin, and cediranib) [38–40]. Moreover, IL-1Ra exhibited a significant effect on the tumor growth dynamics (as assessed by MRI) and survival rates (Figure 3*B*). Our results are reminiscent of previously published data when IL-1Ra was shown to inhibit the development and growth of metastases in mouse B16 melanoma, human cutaneous melanoma xenografts, and uveal melanoma [41–44].

Following assessment of IL-1Ra, we analyzed the theranostic activity of the SPION–IL-1Ra conjugate. The parameters of R_1, R_2, and R_2^* relaxivity for synthesized conjugates were comparable to that of T_2-negative MR contrast agents (Figure 5). As was expected, magnetic nanoparticles were incorporated inside the C6 glioma cells as well as the rats' lymphocytes (Figure 6). The uptake of nanoparticles did not exert the toxic effects on the cells, as was demonstrated with the help of MTT and trypan blue exclusion methods. The i.v. injection of the SPION–IL-1Ra resulted in the retention of the particles in the glioma tissue that was observed at T_2-weighted images and subsequent histologic assay (Figure 7). Previously, it was shown that functionalized particles may penetrate the brain-tumor barrier, enhancing the T_2-weighted MR scans of the brain tumors [19,27,45,46]. Incorporation of magnetic conjugates was displayed as obvious dark regions in the glioma on T_2 scans in comparison to baseline images (on TurobRARE-T2 and FLASH regimens; Figure 7*A*). Application of IL-1Ra increased the tumor retention of the conjugates compared to non-conjugated SPIONs probably due to the IL-1 receptor–mediated targeted delivery of the particles (Figure 6). Moreover, synthesized SPION–IL-1Ra also exerted a therapeutic potential. Thus, accumulation of conjugates resulted in the reduction of the peritumoral edema (as shown on ADC maps) compared to the non-conjugated magnetic particles. Significantly, magnetic conjugates demonstrated biologic anti-edemal therapy at significantly lower concentrations of receptor antagonist (i.e., 2.5 mg/kg) in comparison to the administration of purified protein (when the effect

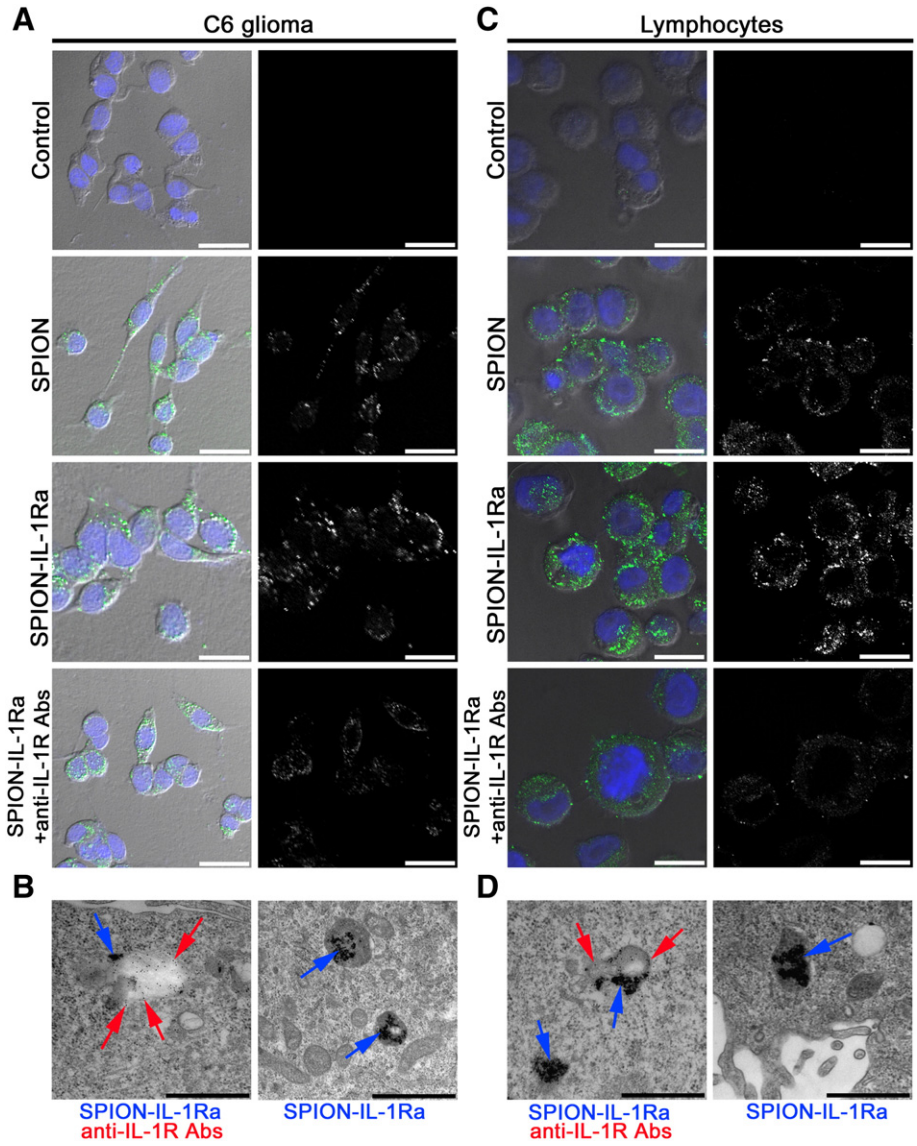

Figure 6. Interaction of the magnetic conjugates of IL-1Ra with C6 cells or lymphocytes. (A) Confocal microscopy images of the C6 cells following 24 hours of incubation with PBS, SPIONs (150 μg/ml), and SPION–IL-1Ra conjugates (150 μg/ml). Nuclei were stained with DAPI (blue). Magnetic nanoparticles were detected by reflecting laser scanning at 488 nm (green). Scale bar, 25 μm. For analysis of the receptor-mediated endocytosis, C6 cells were also incubated with anti–IL-1R monoclonal antibodies. (B) TEM of the C6 cell incubated for 24 hours with SPION–IL-1Ra conjugates. Electron dense nanoparticles were present in the cytoplasm of cells in the endosome-like structures (blue solid arrow). Receptors for IL-1 were detected with monoclonal anti–IL-1R antibodies (red solid arrow). Scale bar, 500 nm. (C) Confocal microscopy images of the rat lymphocytes following 24 hours of incubation with PBS, SPIONs (150 μg/ml), and SPION–IL-1Ra conjugates (150 μg/ml). Nuclei were stained with DAPI (blue). Magnetic nanoparticles are represented in the cytoplasm as green dots. Scale bar, 25 μm. For analysis of the receptor-mediated endocytosis, C6 cells were also incubated with anti–IL-1R monoclonal antibodies. (D) TEM of the lymphocyte incubated for 24 hours with SPION–IL-1Ra conjugates (blue arrows). Receptors for IL-1 were detected with monoclonal anti–IL-1R antibodies (red arrows). Scale bar, 500 nm.

was detected at concentrations of IL-1Ra exceeding 25 mg/kg). Presumably, covalent binding of protein to the nanoparticles may increase the biologic activity of the protein, probably due to molecular interaction between the nanomaterial and the biomolecule [47,48]. Correspondingly, it was shown by Singh et al. that conjugation of the Gαi1 subunit (of heterotrimeric G-proteins) to gold nanoparticles accelerated its GTPase activity five-fold [47]. In addition, the phenomenon of enhanced permeability and retention allows the magnetic nanoparticles to enter the tumor interstitial space, whereas the suppressed lymphatic filtration allows them to stay there [49]. Presumably due to the enhanced permeability and retention effect, SPION–IL-1Ra conjugates remain longer in the glioma tissue than the IL-1Ra protein, thus enhancing the potency of the antagonist in the tumor.

The tumor retention of SPION–IL-1Ra also influenced the survival of the tumor-bearing rats (Figure 7*C*). Thus, we observed a nearly two-fold increase in the life span of those rats treated with SPION–IL-1Ra in comparison to control animals ($P < .001$).

Recombinant IL-1Ra was successfully applied for management of experimental peritumoral edema in the C6 glioma model. The systemic administration of IL-1Ra significantly reduced the edema and exceeded

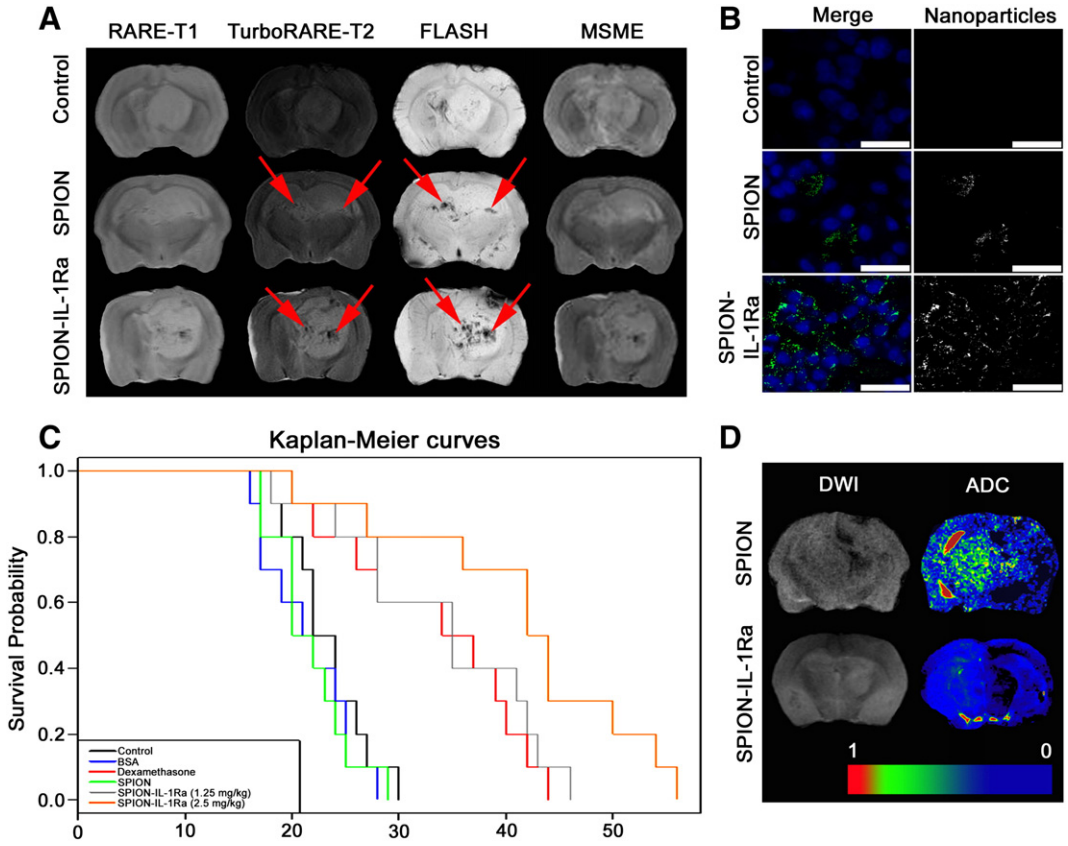

Figure 7. C6 glioma targeting with SPION–IL-1Ra conjugates. (A) MRI of the C6 glioma 24 hours following i.v. treatment with SPIONs or SPION–IL-1Ra conjugates. MR scans were obtained at RARE-T1, TurboRARE-T2, FLASH, and MSME regimens. Retention of the magnetic nanoparticles is presented as hypotensive zones at T_2-weighted images and in the regimen of the gradient echo (red arrows). (B) Confocal microscopy of the C6 glioma sections. Nanoparticles were detected by reflecting laser scanning (green) and nuclei were stained with DAPI (blue). Scale bar, 75 μm. (C) Kaplan-Meier survival curves for the control group and animals treated with BSA, dexamethasone, and SPION–IL-1Ra conjugates at 1.25 and 2.5 mg/kg of IL-1Ra. (D) DWIs and the corresponding ADC maps for the animals treated with SPION or SPION–IL-1Ra conjugates.

the effect of standard dexamethasone therapy. Moreover, IL-1Ra also promoted the survival of animals with reduction of tumor growth rates. Synthesized conjugates of IL-1Ra with superparamagnetic nanoparticles improved the tumor retention of the protein without compromising its biologic activity. The encouraging results of theranostic application of SPION–IL-1Ra conjugates for tumor MR visualization and anti-edemal therapy warrant further study with a view to clinical application of the conjugates in neuro-oncology.

Acknowledgements

The authors are grateful to Irina V. Romanova for assistance in histologic studies; Olga G. Genbach, Nelly V. Koroleva, Dmitriy N. Suslov, Oleg V. Galibin, Tatiana V. Zakoldaeva, Irina V. Kononova, and Yulia E. Shevchuk for assistance in animal experiments.

Appendix A. Supplementary Materials

Supplementary data to this article can be found online at http://dx.doi.org/10.1016/j.neo.2014.11.001.

References

[1] Schoenegger K, Oberndorfer S, Wuschitz B, Struhal W, Hainfellner J, Prayer D, Heinzl H, Lahrmann H, Marosi C, and Grisold W (2009). Peritumoral edema on MRI at initial diagnosis: an independent prognostic factor for glioblastoma? *Eur J Neurol* **16**, 874–878.

[2] Koehler PJ (1995). Use of corticosteroids in neuro-oncology. *Anticancer Drugs* **16**, 19–33.

[3] Dietrich J, Rao K, Pastorino S, and Kesari S (2011). Corticosteroids in brain cancer patients: benefits and pitfalls. *Expert Rev Clin Pharmacol* **4**, 233–242.

[4] Roth P, Regli L, Tonder M, and Weller M (2013). Tumor-associated edema in brain cancer patients: pathogenesis and management. *Expert Rev Anticancer Ther* **13**, 1319–1325.

[5] Badie B, Schartner JM, Hagar AR, Prabakaran S, Peebles TR, Bartley B, Lapsiwala S, Resnick DK, and Vorpahl J (2003). Microglia cyclooxygenase-2 activity in experimental gliomas: possible role in cerebral edema formation. *Clin Cancer Res* **9**, 872–877.

[6] Rinne ML, Lee EQ, Nayak L, Norden AD, Beroukhim R, Wen PY, and Reardon DA (2013). Update on bevacizumab and other angiogenesis inhibitors for brain cancer. *Expert Opin Emerg Drugs* **18**, 137–153.

[7] Zhang X, Cong D, Shen D, Gao X, Chen L, and Hu S (2014). The effect of bumetanide on photodynamic therapy-induced peri-tumor edema of C6 glioma xenografts. *Lasers Surg Med* **46**, 422–430.

[8] Grände PO and Romner B (2012). Osmotherapy in brain edema: a questionable therapy. *J Neurosurg Anesthesiol* **24**, 407–412.

[9] Masada T, Hua Y, Xi G, Yang GY, Hoff JT, Keep RF, and Nagao S (2003). Overexpression of interleukin-1 receptor antagonist reduces brain edema induced by intracerebral hemorrhage and thrombin. *Acta Neurochir Suppl* **86**, 463–467.

[10] Masada T, Hua Y, Xi G, Yang GY, Hoff JT, and Keep RF (2001). Attenuation of intracerebral hemorrhage and thrombin-induced brain edema by overexpression of interleukin-1 receptor antagonist. *J Neurosurg* **95**, 680–686.

[11] Tehranian R, Andell-Jonsson S, Beni SM, Yatsiv I, Shohami E, Bartfai T, Lundkvist J, and Iverfeldt K (2002). Improved recovery and delayed cytokine induction after

closed head injury in mice with central overexpression of the secreted isoform of the interleukin-1 receptor antagonist. *J Neurotrauma* **19**, 939–951.

[12] Girard S, Sébire H, Brochu ME, Briota S, Sarret P, and Sébire G (2012). Postnatal administration of IL-1Ra exerts neuroprotective effects following perinatal inflammation and/or hypoxic-ischemic injuries. *Brain Behav Immun* **26**, 1331–1339.

[13] Pradillo JM, Denes A, Greenhalgh AD, Boutin H, Drake C, McColl BW, Barton E, Proctor SD, Russell JC, and Rothwell NJ, et al (2012). Delayed administration of interleukin-1 receptor antagonist reduces ischemic brain damage and inflammation in comorbid rats. *J Cereb Blood Flow Metab* **32**, 1810–1819.

[14] Bar D, Apte RN, Voronov E, Dinarello CA, and Cohen S (2004). A continuous delivery system of IL-1 receptor antagonist reduces angiogenesis and inhibits tumor development. *FASEB J* **18**, 161–163.

[15] Elaraj DM, Weinreich DM, Varghese S, Puhlman M, Hewitt SM, Carroll NM, Feldman ED, Turner EM, and Alexander HR (2006). The role of interleukin 1 in growth and metastasis of human cancer xenografts. *Clin Cancer Res* **12**, 1088–1096.

[16] Weinreich DM, Elaraj DM, Puhlmann M, Hewitt SM, Carroll NM, Feldman ED, Turner EM, Spiess PJ, and Alexander HR (2003). Effect of interleukin 1 receptor antagonist gene transduction on human melanoma xenografts in nude mice. *Cancer Res* **63**, 5957–5961.

[17] Fuchigami T, Kibe T, Koyama H, Kishida S, Iijima M, Nishizawa Y, Hijioka H, Fujii T, Ueda M, and Nakamura N, et al (2014). Regulation of IL-6 and IL-8 production by reciprocal cell-to-cell interactions between tumor cells and stromal fibroblasts through IL-1α in ameloblastoma. *Biochem Biophys Res Commun* **451**, 491–496.

[18] Greenhalgh AD, Galea J, Dénes A, Tyrrell PJ, and Rothwell NJ (2010). Rapid brain penetration of interleukin-1 receptor antagonist in rat cerebral ischaemia: pharmacokinetics, distribution, protection. *Br J Pharmacol* **160**, 153–159.

[19] Shevtsov MA, Yakovleva LY, Nikolaev BP, Marchenko YY, Dobrodumov AV, Onokhin KV, Onokhina YS, Selkov SA, Mikhrina AL, and Guzhova IV, et al (2014). Tumor targeting using magnetic nanoparticle Hsp70 conjugate in a model of C6 glioma. *Neuro Oncol* **16**, 38–49.

[20] Marchenko YY, Shishkin AN, Yakovleva LY, and Nikolaev BP (2012). The magnetic relaxation platform for biosensing cancer markers: the relaxivity of magnetic nanoparticles conjugated with epidermal growth factor under influence of its antibody. NMRCM 2012, 9th meeting: "NMR in Heterogeneous Systems", St. Petersburg, Russia, July 9–13; 2012. p. 104 [Book of abstracts].

[21] Shevtsov MA, Nikolaev BP, Yakovleva LY, Marchenko YY, Dobrodumov AV, Mikhrina AL, Martynova MG, Bystrova OA, Yakovenko IV, and Ischenko AM (2014). Superparamagnetic iron oxide nanoparticles conjugated with epidermal growth factor (SPION-EGF) for targeting brain tumors. *Int J Nanomedicine* **9**, 273–287.

[22] Fuss IJ, Kanof ME, Smith PD, and Zola H (2009). Isolation of whole mononuclear cells from peripheral blood and cord blood. *Curr Protoc Immunol* . http://dx.doi.org/10.1002/0471142735.im0701s85.

[23] Li M, Deng H, Peng H, and Wang Q (2014). Functional nanoparticles in targeting glioma diagnosis and therapies. *J Nanosci Nanotechnol* **14**, 415–432.

[24] Tzeng SY and Green JJ (2013). Therapeutic nanomedicine for brain cancer. *Ther Deliv* **4**, 687–704.

[25] Urries I, Muñoz C, Gomez L, Marquina C, Sebastian V, Arruebo M, and Santamaria J (2014). Magneto-plasmonic nanoparticles as theranostic platforms for magnetic resonance imaging, drug delivery and NIR hyperthermia applications. *Nanoscale* **6**, 9230–9240.

[26] Wang B, Lu L, Wang Z, Zhao Y, Wu L, Fang X, Xu Q, and Xin H (2014). Nanoparticles functionalized with Pep-1 as potential glioma targeting delivery system via interleukin 13 receptor α2-mediated endocytosis. *Biomaterials* **35**, 5897–5907.

[27] Hadjipanayis CG, Machaidze R, Kaluzova M, Wang L, Schuette AJ, Chen H, Wu X, and Mao H (2010). EGFRvIII antibody-conjugated iron oxide nanoparticles for magnetic resonance imaging-guided convection-enhanced delivery and targeted therapy of glioblastoma. *Cancer Res* **70**, 6303–6312.

[28] Hu Q, Gu G, Liu Z, Jiang M, Kang T, Miao D, Tu Y, Pang Z, Song Q, and Yao L, et al (2013). F3 peptide-functionalized PEG-PLA nanoparticles co-administrated with tLyp-1 peptide for anti-glioma drug delivery. *Biomaterials* **34**, 1135–1145.

[29] Apte RN, Dotan S, Elkabets M, White MR, Reich E, Carmi Y, Song X, Dvozkin T, Krelin Y, and Voronov E (2006). The involvement of IL-1 in tumorigenesis, tumor invasiveness, metastasis and tumor-host interactions. *Cancer Metastasis Rev* **2**, 387–408.

[30] Song X, Krelin Y, Dvorkin T, Bjorkdahl O, Segal S, Dinarello CA, Voronov E, and Apte RN (2005). $CD11b^+/Gr\text{-}1^+$ immature myeloid cells mediate suppression of T cells in mice bearing tumors of IL-1β-secreting cells. *J Immunol* **175**, 8200–8208.

[31] Bunt SK, Sinha P, Clements VK, Leips J, and Ostrand-Rosenberg S (2006). Inflammation induces myeloid-derived suppressor cells that facilitate tumor progression. *J Immunol* **176**, 284–290.

[32] Cawthorne C, Prenant C, Smigova A, Julyan P, Maroy R, Herholz K, Rothwell N, and Boutin H (2011). Biodistribution, pharmacokinetics and metabolism of interleukin-1 receptor antagonist (IL-1RA) using [^{18}F]-IL1RA and PET imaging in rats. *Br J Pharmacol* **162**, 659–672.

[33] Leten C, Struys T, Dresselaers T, and Himmelreich U (2014). In vivo and ex vivo assessment of the blood brain barrier integrity in different glioblastoma animal models. *J Neurooncol* **119**, 297–306.

[34] Watkins S, Robel S, Kimbrough IF, Robert SM, Ellis-Davies G, and Sontheimer H (2014). Disruption of astrocyte-vascular coupling and the blood-brain barrier by invading glioma cells. *Nat Commun* **5**, 4196.

[35] Huang Y, Hoffman C, Rajappa P, Kim JH, Hu W, Huse J, Tang Z, Li X, Weksler B, and Bromberg J, et al (2014). Oligodendrocyte progenitor cells promote neovascularization in glioma by disrupting the blood-brain barrier. *Cancer Res* **74**, 1011–1021.

[36] Nduom EK, Yang C, Merrill MJ, Zhuang Z, and Lonser RR (2013). Characterization of the blood-brain barrier of metastatic and primary malignant neoplasms. *J Neurosurg* **119**, 427–433.

[37] Nowosielski M, Recheis W, Goebel G, Güler O, Tinkhauser G, Kostron H, Schocke M, Gotwald T, Stockhammer G, and Hutterer M (2011). ADC histograms predict response to anti-angiogenic therapy in patients with recurrent high-grade glioma. *Neuroradiology* **53**, 291–302.

[38] Hawkins-Daarud A, Rockne RC, Anderson AR, and Swanson KR (2013). Modeling tumor-associated edema in gliomas during anti-angiogenic therapy and its impact on imageable tumor. *Front Oncol* **3**, 66.

[39] Yang LJ, Lin ZX, Kang DZ, Weng SM, Lin JH, Huang Q, and Zhang PF (2011). Effects of endostatin on C6 glioma-induced edema. *Chin Med J (Engl)* **124**, 4211–4216.

[40] Dietrich J, Wang D, and Batchelor TT (2009). Cediranib: profile of a novel anti-angiogenic agent in patients with glioblastoma. *Expert Opin Investig Drugs* **18**, 1549–1557.

[41] McKenzie RC, Oran A, Dinarello CA, and Sauder DN (1996). Interleukin-1 receptor antagonist inhibits subcutaneous B16 melanoma growth in vivo. *Anticancer Res* **16**, 437–441.

[42] Lavi G, Voronov E, Dinarello CA, Apte RN, and Cohen S (2007). Sustained delivery of IL-1 Ra from biodegradable microspheres reduces the number of murine B16 melanoma lung metastases. *J Control Release* **123**, 123–130.

[43] Triozzi PL and Aldrich W (2010). Effects of interleukin-1 receptor antagonist and chemotherapy on host-tumor interactions in established melanoma. *Anticancer Res* **30**, 345–354.

[44] Triozzi PL, Aldrich W, and Singh A (2011). Effects of interleukin-1 receptor antagonist on tumor stroma in experimental uveal melanoma. *Invest Ophthalmol Vis Sci* **52**, 5529–5535.

[45] Li K, Shen M, Zheng L, Zhao J, Quan Q, Shi X, and Zhang G (2014). Magnetic resonance imaging of glioma with novel APTS-coated superparamagnetic iron oxide nanoparticles. *Nanoscale Res Lett* **9**, 304.

[46] Cui Y, Xu Q, Chow PK, Wang D, and Wang CH (2013). Transferrin-conjugated magnetic silica PLGA nanoparticles loaded with doxorubicin and paclitaxel for brain glioma treatment. *Biomaterials* **34**, 8511–8520.

[47] Singh V, Nair SP, and Aradhyam GK (2013). Chemistry of conjugation to gold nanoparticles affects G-protein activity differently. *J Nanobiotechnology* **11**, 7.

[48] Saptarshi SR, Duschl A, and Lopata AL (2013). Interaction of nanoparticles with proteins: relation to bio-reactivity of the nanoparticle. *J Nanobiotechnology* **11**, 26.

[49] Prabhakar U, Maeda H, Jain RK, Sevick-Muraca EM, Zamboni W, Farokhzad OC, Barry ST, Gabizon A, Grodzinski P, and Blakey DC (2013). Challenges and key considerations of the enhanced permeability and retention effect for nanomedicine drug delivery in oncology. *Cancer Res* **73**, 2412–2417.